Published in final edited form as:
NMR Biomed. 2008 November ; 21(9): 941–956. doi:10.1002/nbm.1230.

MRI in ocular drug delivery

S. Kevin Li[1,*], **Martin J. Lizak**[2], and **Eun-Kee Jeong**[3]

[1]Division of Pharmaceutical Sciences, College of Pharmacy, University of Cincinnati, Cincinnati, OH 45267, USA

[2]National Institute of Neurological Disease and Stroke, National Institutes of Health, Bethesda, MD 20892, USA

[3]Department of Radiology and Utah Center for Advanced Imaging Research, University of Utah, Salt Lake City, UT 84108, USA

Abstract

Conventional pharmacokinetic methods for studying ocular drug delivery are invasive and cannot be conveniently applied to humans. The advancement of MRI technology has provided new opportunities in ocular drug-delivery research. MRI provides a means to non-invasively and continuously monitor ocular drug-delivery systems with a contrast agent or compound labeled with a contrast agent. It is a useful technique in pharmacokinetic studies, evaluation of drug-delivery methods, and drug-delivery device testing. Although the current status of the technology presents some major challenges to pharmaceutical research using MRI, it has a lot of potential. In the past decade, MRI has been used to examine ocular drug delivery via the subconjunctival route, intravitreal injection, intrascleral injection to the suprachoroidal space, episcleral and intravitreal implants, periocular injections, and ocular iontophoresis. In this review, the advantages and limitations of MRI in the study of ocular drug delivery are discussed. Different MR contrast agents and MRI techniques for ocular drug-delivery research are compared. Ocular drug-delivery studies using MRI are reviewed.

Keywords

MRI; eye; ocular; drug delivery; contrast agent

INTRODUCTION

MRI pharmacokinetic studies

Recent advances in imaging and spectroscopy technologies have provided new opportunities for pharmaceutical scientists to study the delivery of drugs and drug-delivery systems *in vivo*. These new methods, such as confocal Raman spectroscopy (1), X-ray computed tomography (2), electron paramagnetic resonance spectroscopy (3), molecular imaging (4,5), positron emission tomography, single photon emission computed tomography (6), and MRI (7-10), are particularly useful for non-invasive monitoring of drug distribution in the body in drug-delivery research. For example, MRI has been used to retrieve real-time data on the delivery, distribution, and elimination of drugs and drug-delivery systems. In oral drug-delivery research, MRI has been used to study the behavior of intragastric olive oil emulsions

*Correspondence to: S. K. Li, Division of Pharmaceutical Sciences, College of Pharmacy, University of Cincinnati, Cincinnati, OH 45267, USA. E-mail: kevin.li@uc.edu

and gastric emptying of the emulsions in human gastrointestinal tract (11). Recent MRI studies in drug delivery also include monitoring of drug carriers such as liposomes, micelles, nanoparticles, and synthetic polymers when the carriers are loaded or labeled with manganese (Mn) or gadolinium (Gd) probes. Viglianti *et al*. (12) investigated the feasibility of MRI for monitoring liposomes in targeted drug delivery. The distribution and tissue concentration of $MnSO_4$-loaded liposomes during and after administration were determined in rats. Port *et al*. (13) studied the release of a hydrophilic drug from an interstitial depot of liposomes subcutaneously administered to rats *in vivo*, and the release of the drug and contrast agent from the liposomes was monitored by ^{19}F MRS and contrast-enhanced MRI. In addition to liposome targeted drug delivery, MRI has been used to non-invasively monitor the delivery and release kinetics of biodegradable and bioadhesive polymeric microparticles such as in the study of local distribution and degradation of contrast agent-encapsulated polymeric particles at the sites of administration *in vivo* (14). The pharmacokinetics and distribution of paramagnetically labeled polymers of different molecular sizes have been visualized by MRI in mice *in vivo*, and the efficiency of targeting of polymer to tumors has been assessed (15,16). Kayyem *et al*. (17) studied the delivery of DNA-bound polylysine-conjugated particles with MRI. In traditional drug delivery, MRI has been used to assist intraparenchymal injections and to obtain three-dimensional (3D) data on the distributions in organs and tissues (18). Iontophoretic drug delivery to the tympanic membrane and middle and inner ear has also been examined using MRI (19,20). In addition, MRI has been used in vaginal drug-delivery studies to determine the distribution of a vaginal gel and the effects of, for example, its volume on distribution by loading the gel with a contrast agent (21).

Problems with conventional ocular pharmacokinetic studies

Successful development of novel ocular drug-delivery methods as well as improvements in the existing drug-delivery techniques depend on the availability of reliable ocular pharmacokinetic data. The lack of understanding of ocular drug-delivery mechanisms, pharmacokinetics, distribution, and elimination is partly due to the complicated anatomy of the eye (22,23). It is also a result of the lack of data because of the invasive approaches taken to study ocular drug distributions. Conventional ocular pharmacokinetic studies are invasive and severely perturb the eye during sampling. In animal studies, it involves killing the animals at different time points after drug administration and assaying different sections of the eye for the drug. It is inconvenient and expensive, and requires a large number of animals in each study. Sampling of the eye by dissection in traditional pharmacokinetic studies can also result in the redistribution of the compound of interest in the eye and cross-contamination among the tissues during assay. The extent of these problems increases with decreasing animal size. In addition, these traditional methods are not readily applicable to healthy human subjects. For example, ocular pharmacokinetic studies in humans are uncommon and are mostly performed in conjunction with clinical eye operations such as vitrectomy (24-27).

Ocular drug-delivery studies using MRI

The use of MRI to determine the distribution and route of elimination of ions and compounds during and after ocular drug delivery has many advantages. Unlike traditional pharmacokinetic techniques used to study ocular drug delivery and drug pharmacokinetics, MRI is non-invasive. Because MRI is non-invasive, the number of experiments and experimental animals required can be greatly reduced. This approach also allows real-time determination of the distribution pattern (or concentration profile) of the compound of interest in the eye. Such refined distribution profiles would be difficult to determine in conventional ocular pharmacokinetic studies. In addition, MRI can provide insights into ocular pharmacokinetics without tissue perturbation and redistribution of the compound, which could occur with conventional dissection methods. Another advantage of MRI is its potential for use in human ocular research. Table 1 summarizes the differences, advantages, and disadvantages of non-invasive ocular

drug-delivery studies with MRI and the traditional ocular pharmacokinetic studies with the technique of dissection. Figure 1 provides examples of recent MRI studies of ocular drug delivery.

The intent of this paper is to give a general overview of MRI in drug-delivery research, particularly, ocular drug delivery. MRI ocular drug-delivery research is multidisciplinary, requiring familiarity with ocular drug delivery and MRI technology. An objective therefore is to provide both pharmaceutical researchers and MRI scientists with the necessary knowledge to understand and perform MRI studies on ocular drug delivery. This review will discuss the advantages and limitations of MRI in ocular drug-delivery research. A brief review of MRI techniques, MR contrast agents, and MRI methods for ocular drug delivery will be provided. Then ocular drug-delivery studies that have used MRI will be reviewed.

TECHNICAL CHALLENGES

Challenges of ocular drug delivery

Ocular drug delivery can be classified according to the anatomy of the eye: delivery to the anterior and posterior segments. For the anterior segment of the eye, topical administration, although ineffective and sometimes inconvenient, is the most common form of treatment. In general, less than 7% of the drug administered as eye drops reaches the aqueous humor because of the corneal and conjunctival barriers and precorneal clearance such as tear drainage (28, 29). To improve topical drug delivery to the anterior segment of the eye, devices and sustained-release drug-delivery systems such as collagen shields, lenses, and emulsions have been investigated (30-33). Systemic drug delivery can also be used but is limited by systemic toxicity and the blood-aqueous barrier at the ciliary body (28).

Another challenge is to deliver a drug to the posterior segment of the eye in the treatment of posterior eye disease. Drugs do not usually reach this part of the eye at therapeutic concentrations after the administration of eye drops because of the anatomical and physiological barriers of the eye. For example, after a drug reaches the anterior chamber, it is eliminated from the aqueous chamber through Schlemm's canal and capillary in the anterior uvea. Transscleral drug delivery has also been suggested to be an effective route of drug delivery to the back of the eye (34), but this route is hindered by barriers, such as the conjunctiva and sclera, and clearance, such as conjunctival and choroidal vasculature clearance (29,35). These barriers have presented an obstacle to drug delivery for the treatment of posterior eye diseases (36).

Two common routes of treatments for posterior eye disease are direct injection (intravitreal and periocular) and systemic drug administration. Frequent injections may cause complications such as retinal detachment, and systemic drug administration is not effective because of the blood-retina barrier and systemic toxicity (28). Recent developments in ocular drug delivery in the treatment of posterior eye diseases include: injection of drug-encapsulated liposome/polymer delivery systems or drug suspensions into the subconjunctival or suprachoroidal space (37,38); biodegradable and non-biodegradable surgical implants in the vitreous or other parts of the eye for diseases such as postoperative inflammation, macular edema, cytomegaloviral retinitis, and posterior uveitis (39-42); a periocular cannula delivery system for macular degeneration (43); and iontophoresis for different eye diseases (44). The transscleral route has also been explored (34). Although there have been intense efforts to develop new drug-delivery systems to the posterior segment of the eye, some important questions remain. For example, the interplay between the ocular barriers and the distribution and clearance of drugs in ocular drug delivery is not completely understood. Factors such as the effects of molecular size, charge, and lipophilicity of the drug, diffusion in the vitreous humor (45), kinetics between the posterior and anterior chambers, clearance in the anterior chamber and vitreous humor (46),

permeation across the sclera, choroid, and retina (47,48), and dynamic barriers (49), such as blood and lymphatic clearance, in ocular drug delivery have not been well studied.

Review of MRI techniques

MRI principles and techniques—Most MRI techniques are based on either spin-echo (SE) or gradientecho (GRE) pulse sequences. The SE technique gives the best weighted images for the T_1 and T_2 contrasts, where T_1 and T_2 are the spin-lattice (or longitudinal) and spin-spin (or transverse) relaxation times, respectively. SE images are also easy to quantify, but SE requires a relatively long imaging time (slow). Methods such as multiple SE pulse sequences (fast or turbo SE) can speed up the acquisition and improve the signal-to-noise ratio (SNR). The GRE imaging method utilizes steady-state magnetization and low excitation (flip angle) to speed up the acquisition. The imaging contrast of GRE is less straightforward than SE imaging, because of its T_2* effect. T_2* is an additional transverse relaxation time, which is greatly influenced by local non-uniformity of the magnetic field rather than the true spin-spin interaction in T_2. T_2* of tissue water is generally much shorter than the spin-spin relaxation time T_2. The resulting images generally have mixed T_1 and T_2* contrast, particularly in dynamic contrast-enhanced MRI, because these relaxation times change rapidly due to the change in the local concentration of the contrast agent. The choice of the imaging method depends on how fast the concentration of the contrast agent changes in the tissues of interest. Because drug movement in ocular drug delivery usually relies on passive diffusion across tissues (rather than high velocity convection such as in blood), the local concentration varies slowly. Therefore, a SE pulse sequence is preferred in ocular drug-delivery and pharmacokinetic studies.

Methods of SE MRI and ocular drug-delivery research—In general, the signal intensity of the voxels in SE imaging can be described by:

$$S\,(TR,TE) = S_0\left(1 - 2e^{-(TR-0.5TE)/T_1} + e^{-TR/T_1}\right)\cdot e^{-TE/T_2} \quad (1)$$

where *S(TR,TE)* or *S* is the signal intensity, S_o is the intrinsic fully recovered signal intensity, *TR* is the repetition time, and *TE* is the echo-time. For typical T_1-weighted imaging with $TR \gg TE$, eqn (1) can be simplified as:

$$S\,(TR,TE) = S_0\left(1 - e^{-TR/T_1}\right)\cdot e^{-TE/T_2} \quad (2)$$

The contrast between tissues with different T_1 relaxation times increases with decreasing *TR*. However, decreasing *TR* reduces the signal intensity. *TR* is usually kept around 400 ms for T_1-weighted imaging of biological MRI (e.g. at 1.5 T) for reasonable imaging time and spatial resolution. *TE* also affects the MRI results. The choice of the minimum *TE* is essential to obtain the best T_1 weighting (with the least T_2 weighting) as well as to increase SNR. Eqn (2) is also used in SE MRI studies with a contrast agent. Contrast agent-enhanced MRI works by the principle that the contrast agent enhances the relaxivity of the surrounding protons. In general, the relaxation rates, $1/T_1$ and $1/T_2$, of the protons increase linearly with the concentration of the contrast agent. The relationship between signal intensity and contrast agent concentration is therefore non-linear. In T_1-weighted MRI, as the concentration of the contrast agent increases, the signal intensity increases, reaches a maximum value, and then decreases after the maximum. Figure 2a shows the relationships between relaxation rates and concentration of the contrast agent. The relationships between S/S_o and contrast agent concentration and the effects of *TR* and *TE* are illustrated in Fig. 2b (see eqn 2).

Two methods are commonly used to determine the concentration of a contrast agent in the eye: (a) comparison of MR signal intensity with a calibration standard and (b) T_1 and T_2 measurement. Direct determination of the concentration of contrast agent using MR signal intensity with a calibration standard is the more convenient method but is prone to experimental errors such as variability of the position of the eye with respect to the radio-frequency (RF) coil (these errors will be further discussed under 'Sources of errors in MRI ocular drug-delivery studies'). These studies are usually performed using the contrast agent at or below the concentration of maximum S/S_o to avoid complications in data interpretation. Higher concentrations can be used, but a strategy to determine if the signal is on the increasing or decreasing end of the peak in the S/S_o vs concentration plot of Fig. 2b should be implemented.

T_1 and T_2 measurements can avoid the experimental errors involved in direct MR signal measurements to determine the concentration of a contrast agent. The conventional method used to calculate T_1 and T_2 is curve fitting of the signal intensity of a region of interest (ROI) with respect to the time variables *TE* and *TR* using eqn (2). In this case, T_1 of the MR signal can be measured by varying *TR* and fixing *TE*. T_2 are measured by varying *TE* and fixing *TR*. Because a series of MR scans of different *TR* and *TE* settings are required in T_1 and T_2 determination, this method is time-consuming. T_1 and T_2 measurements are therefore not preferred when temporal resolution is an important factor. Fast imaging methods such as GRE imaging with multiple flip angles (50) or segmented echo-planar imaging with automated variation of *TR* and *TE* (51) may be used to overcome this limitation.

In data analysis, the MR images obtained at different time points are used to provide a real-time concentration profile of the test compound (e.g. contrast agent) in the eye after administration. The effectiveness of an ocular drug-delivery method, diffusion paths, and ocular barriers can then be evaluated. In addition to pharmacokinetic compartment model analyses (23,48), the concentration profile can be modeled using finite element analysis (45, 52,53) to determine ocular drug-delivery parameters such as diffusion coefficients, tissue permeability coefficients, and convective flow rate, based on the diffusion and convection equation of the second Fick's law:

$$\frac{\partial C}{\partial t} = \nabla (D \nabla C + vC) \tag{3}$$

where C is the concentration, t is time, D is the diffusion coefficient, and v is the velocity vector. The combination of a finite element method and MRI is a powerful tool in ocular drug-delivery studies. Fig. 3a shows a typical study of the distribution of a contrast agent after it was delivered into a rabbit eye *in vivo*. Fig. 3b is an example of the result from a finite element model simulation of diffusion from the site of administration into the eye. Such analyses of ocular distribution in ocular drug delivery would be difficult to achieve without MRI.

Limitations of MRI in ocular drug-delivery studies—Although MRI is a promising technique in ocular drug-delivery research, it has limitations. First, the sensitivity of the existing MRI technology is a limiting factor. Spatial and temporal resolutions are important in ocular drug-delivery research with MRI. To provide a quantitative perspective, the spatial resolutions of MRI in recent ocular drug-delivery studies (~0.3 mm, in-plane) are of the same order of magnitude as small ocular structures such as the retina, which may not allow the visualization of the contrast agent in these structures. Figure 4a shows a MR image of 0.47 mm × 0.47 mm × 2 mm voxel resolution. As can be seen in the MR image, the spatial resolution of this particular MR protocol does not allow clear distinction of some eye structures. When the spatial resolution increases, MRI scan time is increased to keep the same SNR at the higher spatial resolution. SNR does not increase linearly with MRI scan time, but is proportional to the square root of

scan time. For instance, to increase the resolution from 0.5 mm to 0.25 mm in all three dimensions, the scan time needs to be 64 times longer to keep the same SNR without other modifications. Figure 4b shows the MR image of 0.3 mm × 0.3 mm × 1 mm voxels. The spatial resolution of this MR image is significantly enhanced under this MRI protocol, and some eye structures become distinguishable compared with those in Fig. 4a. In addition to sacrificing the temporal resolution, long scan times are also more likely to introduce motion artifacts. Figure 4c,d demonstrates the effects of motion artifacts. Most MRI scans in recent ocular drug-delivery studies have (in-plane) spatial resolution of ~0.2-0.5 mm and scan times of ~1-30 min. For example, the scan times for the MR images in Fig. 4a,b are ~1.5 and 20 min, respectively. These scan times can provide sufficient temporal resolution for ocular drug-delivery research. Besides lengthening the scan time, MRI spatial resolution can be improved by other methods. MRI scanners of higher magnetic field can be used to increase MR signals. This allows an increase in SNR or an increase in the MRI spatial resolution at the same SNR (such as in the example of Fig. 4a,b). Signal intensity increases roughly linearly with the increased static magnetic field strength when all other imaging parameters and hardware, including the coil function, are identical. The exact relationship is a little more complicated and is related to the NMR properties of the molecules of interest. For example, T_1 of proton in water increases with field strength, which causes a decrease in the signal in T_1-weighted MRI. A smaller, more sensitive receiving RF coil can be used to obtain greater detail of the eye. However, small surface coils lack the homogeneity of the larger volume coils, so they are prone to errors caused by body movement and sensitivity roll-off. Related to spatial resolution, effects of partial-volume averaging can be significant in ocular drug-delivery studies with MRI. As the dimensions of some ocular tissues, such as the cornea, sclera, choroid, and retina, are comparable to the spatial resolution in typical MRI, particularly SE MRI, and because of the curvature of these tissue layers, the MR slices close to the center of the eye or perpendicular to the tissue layer are more reliable in determining the MR signal of the tissue. The effects of partial-volume averaging can be significant at other locations (Fig. 5). This limits the ability of MRI to determine the concentration of contrast agent in thin tissues across the eye in 3D (in a single SE MRI scan) in ocular pharmacokinetic studies.

Secondly, the current status of MRI requires the use of contrast agent or contrast agent- labeled compounds as surrogates of the actual drug in MRI studies. If the drug or drug-delivery system contains ^{19}F atom, an alternative is to monitor ^{19}F instead of ^{1}H (54). ^{19}F NMR, MRS, and MRI have been used in a variety of studies that are not related to the eye such as antibiotic and chemotherapeutic pharmacokinetics (55,56), blood oxygen tension (57), distribution of an anesthetic (58), and tumor imaging of anticancer drug (59). ^{19}F experiments have also been performed in the eye (60) and in aqueous humor assay (61). If the drug or drug-delivery system does not contain ^{19}F, they can be labeled with ^{19}F (this will be discussed below under ‘MRI contrast agents for ocular drug-delivery research’). Although ^{19}F MRS and MRI are promising methods, the ^{19}F technique at its current stage is not sensitive enough for imaging in ocular drug-delivery research. The concentration of ^{19}F can be several orders of magnitude lower than ^{1}H. In this case, only localized ^{19}F spectroscopy of large voxels can be used. In addition, ^{19}F MRI/MRS capability is not available in most whole-body clinical MRI systems. Even if a clinical scanner is equipped with a broadband RF channel for non-proton MRI/MRS, some hardware development is generally required, such as the RF interface that includes the transmit/receive switching and RF coil. This can be challenging.

Thirdly, the relaxation times of protons in tissues are generally different from those in aqueous medium (e.g. vitreous humor) (62). In T_1-weighted images, some structures in the eye show higher signal intensities (e.g. the cornea, sclera/retina, ciliary body) than the background signal of water. The effects of contrast agents on tissue MR signals (i.e. tissue T_1 and T_2) are also different in different tissues (63). Quantification of the effects of contrast agents on MR signals in aqueous medium and tissues is therefore required for the interpretation of data and accurate

measurement of the concentration of contrast agents in eye tissues. Control experiments are also needed to identify possible binding of the contrast agent to eye tissues. Without these control and calibration experiments, quantitative MRI analyses are mostly limited to the vitreous and aqueous humor in ocular drug-delivery studies with MRI.

The size of the bore of an MRI scanner can also be a limiting factor in ocular drug-delivery studies that require the use of large animals. Animal scanners with high magnetic field usually have small magnet bores, which cannot accommodate animals larger than rodents. High-field scanners with 'large' bores (such as high-field clinical scanners of 7 T and high-field animal scanners of 30 cm bore) are not common. The availability of these high-field scanners limits the progress of MRI in ocular drug-delivery research because of the applicability of the data obtained with small-animal eyes to human eyes. For instance, the anatomy and dimensions of the animal eyes (such as the distance between the anterior chamber and the retina) are different from those in humans. This can affect ocular drug disposition and pharmacokinetics because the physics of diffusion such as diffusion coefficients are constant, independent of the size of the animal used. If it takes 20 h for a drug to diffuse across human vitreous humor, it will take only 0.5 h for it to diffuse across rat vitreous humor. The properties of the tissue barriers (such as thickness) in animal eyes can also be different among different animal species. For example, human sclera is more than twice as thick as rat sclera. The composition of vitreous humor in humans and animals is also different. When a drug is observed to be delivered to its target site in the eye, such as the retina, with a drug-delivery method in small animals, it is difficult to predict if the method would be effective in humans. Compared with small animals, larger animals are more likely to provide results that are more representative of the situation in humans. However, ocular drug-delivery MRI studies with large animals require the use of scanners with large magnet bore size (such as clinical scanners), and these scanners usually have lower magnetic field than small-animal scanners.

Sources of errors in MRI ocular drug-delivery studies—Because of the quantitative nature of pharmacokinetic studies, ocular drug-delivery research with MRI requires accurate determination of the concentration of the compound of interest. Unlike diagnostic and functional MRI and MRI in anatomical studies, errors in MR signal intensities are more likely to affect the conclusions in ocular drug-delivery studies. Possible sources of errors in MRI are discussed here.

The RF coil spatial sensitivity can be a significant source of error in determining the concentration of contrast agent, in particular, when a surface RF coil is used. In a clinical MRI system, a large body volume RF coil is used for RF transmission to achieve uniform RF excitation, and a surface coil (or array) is used for signal reception. The surface RF coil limits the noise power that is generated from the thermal electronic fluctuations far from the coil and the imaging volume of interest, and therefore is suitable for MRI/MRS of the anatomy located near the surface. When an RF surface coil is used, the coil is usually placed as close as possible to the ROI to achieve higher MR signal intensity. However, the RF field strength as well as the signal detection sensitivity of a surface coil change dramatically with the relative position of the ROI to the coil. This non-uniform spatial sensitivity may impose errors in the quantification of the contrast agent in ocular drug-delivery studies, particularly in the study using the signal intensity as the direct marker of the concentration of the contrast agent. These errors may be reduced by using an array of many small surface coils especially designed for ocular MRI. Correction methods to improve image uniformity are also available (64). In addition, the construction of a device to fix the location of the coil and maintain the relative position between the coil and the ROI (the test subject) during and between experiments can minimize variability and improve MRI reproducibility. Coil inhomogeneity can be tested, and the effects of coil positioning with respect to the ROI on MR signals can be determined in calibration experiments with MRI phantoms.

Another potential source of errors, which are usually minor, is the temperature effect. MRI signal depends on T_1 and T_2 as well as on the physical (translational) diffusion of the water molecules in the tissue (65,66). These NMR parameters change with temperature. For example, the temperature gradient across an eye may affect the measured signal intensity. T_1 and T_2 mappings may reduce such errors by directly measuring the relaxation times. However, the imaging time for T_1/T_2 mapping using the conventional SE or fast SE imaging techniques is long, as discussed above.

MRI contrast agents for ocular drug-delivery research

Selection of contrast agent—Common contrast agents that have been used in drug-delivery research are Mn^{2+}-, $MnEDTA^{2-}$, $GdDTPA^{2-}$, and Gd-labeled polymers, and Gd-labeled proteins. These contrast agents may have different physicochemical properties and tissue kinetics from the drugs used to treat eye diseases. In particular, most contrast agents are charged or hydrophilic and therefore are not effective probes for studying the distributions of lipophilic compounds in ocular drug delivery. In addition, there can be specific interactions between the contrast agent and eye tissues. These interactions include specific tissue binding and tissue uptake of the contrast agent, which can affect the clearance of the agent. In this case, data interpretation should be limited to the delivery of the agent to the tissues and not its clearance, because the applicability of the tissue clearance data to other compounds can be compromised. Specific transport pathways across eye tissues, such as ion channels or membrane transporters for the contrast agent, can also alter the passive permeation pattern of the agent in the eye. When such contrast agents are used as MRI probes in ocular pharmacokinetic studies, caution must be exercised to prevent over-interpretation of the data.

A good contrast agent probe in ocular drug-delivery studies should be stable and not degrade after it has been administered *in vivo*. A stable MRI contrast probe allows the correct assessment of the effects of physiochemical properties (e.g. molecular size and charge) of a compound on its elimination and distribution in the eye. Importantly, the contrast agent should also provide high MR signal enhancement, so it can be easily detected in the eye with MRI. A contrast agent providing high sensitivity for MRI detection is essential in drug-delivery research, as the permeability of the drug-delivery barrier is generally low. For example, if the detection limit of a contrast agent is 0.1 mM and the permeability coefficient of a tissue barrier (P) is 10^{-4} cm/s, a concentration of contrast agent higher than 10 mM is required to provide the diffusion driving force (67) so that the permeation of the contrast agent across the tissue barrier can be detected within reasonable time:

$$J = -D\frac{\partial C}{\partial x} + vC \tag{4}$$

$$J = \frac{1}{A}\frac{dQ}{dt} = PC \quad \text{at steady-state under sink condition} \tag{5}$$

where J is the flux, x is the position in the x-direction, Q is the amount transported across the barrier, and A is the diffusional area. Note that the permeability coefficients of the sclera and retinal epithelium for polar compounds are lower than 10^{-4} cm/s. When a high concentration of contrast agent is used to overcome the detection limit problem, the parabolic relationship between MR signal intensity and contrast agent concentration in SE imaging can complicate the data analysis (see 'Methods of SE MRI and ocular drug-delivery research'). The use of high concentration of contrast agent may also lead to tissue damage, altering the ocular barriers.

Table 2 lists a number of potential contrast agents for ocular drug-delivery studies with MRI. The following is a brief description of selected contrast agents from this list.

Small contrast agents—Mn^{2+} is paramagnetic and has a molecular mass of 55 Da. It has a charge number of 2+ and was one of the first contrast agents used in MRI (68). It is a neuronal contrast agent that can be used to study the structure of the brain, trace the neutronal tract, and monitor neuronal function (69). Examples of these studies are imaging of the liver (70) and neuroaxonal tracing of the optic nerve (71). In ocular pharmacokinetic studies, Mn^{2+} can be taken up by the retinal ganglion cells and transported along the optic axon *in vivo* (72). The rate of transport of Mn^{2+} along the optic axon has been found to be ~0.28 cm/h (71) and can affect the distribution of Mn^{2+} in tissues such as the retina. When Mn^{2+} is used in ocular drug-delivery study, interpretation of the Mn^{2+} results should be limited to Mn^{2+} in the vitreous humor and anterior chamber. Mn^{2+} is small and has been used as a probe to study the distribution of small ions and the pathways of ion transport in ocular iontophoretic delivery (73). In addition, diffusion of small ions in the vitreous and aqueous humor has been investigated by monitoring Mn^{2+} distribution in these compartments in the same study.

Contrast ions can be chelated to reduce contrast agent toxicity and tissue interactions. Mn-chelates, such as the Mn-EDTA complex ($MnEDTA^{2-}$), and Gd-chelates, such as the Gd-diethylenetriaminopenta-acetic acid complex ($GdDTPA^{2-}$ or gadopentetate dimeglumine), are contrast agents that have been used in MRI pharmacokinetic studies. Other examples of chelated Gd contrast agents are Gd-1,4,7,10-tetra-azacyclododecane-1,4,7,10-tetra-acetic acid (gadoterate meglumine), Gd-diethylenetriamine penta-acetic acid bismethylamide (gadodiamide), and Gd-10-(2-hydroxypropyl)-1,4,7,10-tetra-azacyclododecane-1,4,7-triacetic acid (gadoteridol). These complexes are relatively stable because the binding constants between the contrast ion and chelate are generally of the order of 10^{14} to 10^{25} M^{-1} (74,75). However, the possibility of ion-chelate complex dissociation in tissues should not be overlooked. It should also be noted that chelating agents such as EDTA can interact with tight junctions of epithelial cells and enhance paracellular transport (76,77), which may interfere ocular pharmacokinetics; some pharmaceutical contrast agent products contain excess free chelating agents. $GdDTPA^{2-}$ is a paramagnetic contrast agent (78) and is available as an FDA-approved injectable agent (Magnevist; Bayer, Wayne, NJ, USA) in MRI diagnoses. It has a charge of 2- and molecular mass of 546 Da. Overall, because of the molecular size and hydrophilicity of these chelated contrast agents, they do not readily permeate the tight junctions of endothelium such as the blood/brain barrier. These contrast agents are similar in molecular size to small-molecule therapeutic agents. They are highly hydrophilic and have molecular charges similar to those of phosphate prodrugs, making them good surrogate compounds of corticosteroid prodrugs such as dexamethasone phosphate and triamcinolone phosphate.

Another method for investigating ocular pharmacokinetics with MRI is labeling the drugs of interest or drug-delivery systems with a chemical moiety that can be visualized by MRI. Although drugs can be labeled with an MRI contrast agent, the characteristics of the resulting drugs are likely to be different from those of the parent drug compounds. This is because a chelated contrast-ion complex of large molecular size is usually involved in the labeling process. The addition of the bulky MRI contrast moiety to drug compounds affects their charge and hydrophilicity. This strategy of contrast labeling is not suitable for small molecules. It is more appropriate for macromolecules or drug-delivery systems in the study of their distribution and clearance in the eye. In the case of fluorine-labeling, this method does not affect the physicochemical properties of drug molecules as much as the labeling of chelated contrast ion, but, because of the low concentration of ^{19}F, the low signal sensitivity obtained in ^{19}F MRI and ^{19}F MRS can be an issue, (as discussed under ‘Limitations of MRI in ocular drug-delivery studies’).

Other contrast agents—In addition to small contrast agent probes, ocular drug-delivery systems and macromolecules can be labeled properly with contrast agents (79,80) for MRI monitoring of their distribution in drug-delivery studies. For example, Gd-labeled albumin (81) can be used as a surrogate for the delivery of polypeptides. One of the Gd-labeled albumin products is Galbumin (BioPAL, Worcester, MA, USA), which has 10-15 Gd atoms per albumin unit, a charge of -27, and molecular mass of approximately 70 kDa. This is approximately the size of antigen-binding fragments (Fab) of antibodies to vascular endothelial growth factor (VEGF) such as Lucentis (Genentech, San Francisco, CA, USA). Contrast agent-labeled polymers and copolymers of different molecular size and charge (16,82) can also be used to study the effects of these macromolecule parameters on the distribution and clearance of macromolecules in the eye after ocular administration. These polycations, polyanions, and uncharged polymers are good surrogates of macromolecules such as oligonucleotides in MRI ocular drug-delivery research. Oligonucleotides are an important class of therapeutic compounds such as anti-VEGF inhibitors similar to Macugen from OSI EyeTech (Melville, NY, USA). In addition to Gd labeling, macromolecules and drug-delivery systems can also be labeled with ^{19}F in ^{19}F imaging (83).

Another type of contrast agent is iron oxide (84-86). For example, superparamagnetic iron oxide particles can be visualized in T_2-weighted imaging *in vivo*. They are commonly used in the imaging of macrophage activity in liver and lymph nodes in tumor research and diagnoses. Examples of iron oxide nanoparticles are ferumoxides, ferumoxtran, ferumoxsil, and ferumoxytol (Advanced Magnetics, Cambridge, MA, USA). These particles are relatively large compared with small contrast agents but are smaller than microparticulate colloids. They may be used in ocular drug-delivery studies of nanoparticles with MRI, resembling drug-delivery carriers of similar size.

OCULAR DRUG-DELIVERY STUDIES WITH MRI

Table 3 summarizes the discussion in the previous sections on MRI techniques in ocular drug-delivery studies. Examples of such studies will now be provided. The usefulness and potential of MRI in ocular drug-delivery research will be demonstrated.

Several MRI methods have been used to study the transport barriers and mechanisms of ocular drug delivery. One method is to determine the physiological factors, such as the flow dynamic of the aqueous humor and the blood-aqueous and blood-retina barriers, that control drug pharmacokinetics in the eye. An understanding of these factors can provide important insights into drug distribution and clearance during and after ocular delivery. The effectiveness of a drug-delivery method can also be evaluated by monitoring the pharmacological effects of the drug with MRI. An example is monitoring the blood-retina barrier function with intravenously injected contrast agent and MRI after drug administration. Another type of ocular drug-delivery study with MRI is the use of a contrast agent as an MRI probe in place of a drug. As discussed above, most drugs cannot be directly visualized by MRI. This method indirectly monitors drug pharmacokinetics by following the distribution of a surrogate probe. A main drawback is that the surrogate probe may have different physicochemical properties and ocular pharmacokinetics from the drug. However, direct monitoring of the distribution and clearance of the probe with dynamic MRI can provide useful data in the assessment of an ocular drug-delivery method or drug-delivery device. Table 4 summarizes these three types of study in ocular drug-delivery MRI research which are now reviewed.

Measurement of physiological factors and variables

For the anterior segment of the eye, the dynamics of aqueous humor, in the anterior chamber have been investigated using MRI with contrast agents. This is generally accomplished by following the pharmacokinetics of a contrast agent in the aqueous humor. For example,

Kolodny *et al.* (87) used $GdDTPA^{2-}$ to examine the anterior protein pathway in rabbit eyes by contrast-enhanced MRI. The movement of water in the anterior segment of rabbit eye and the aqueous humor dynamics have also been visualized with contrast agents with MRI *in vivo* (88-90). Besides these animal studies, Bert *et al*. (91) have examined the anterior diffusional pathway of solutes in human eye using contrast-enhanced dynamic MRI. The effects of pilocarpine on the blood-aqueous barrier have also been assessed (92). The applicability of MRI in human studies is a major advantage of this technique. With appropriate MRI contrast agents, these methods can provide important new insights into the characteristics of barriers, such as the blood-aqueous barrier, and clearance in the anterior chamber. However, an important assumption of this method is that. The clearance of contrast agents and water in aqueous humor are the same. Aqueous humor pharmacokinetics can depend on molecular size. The difference between clearance of contrast agent and drainage of aqueous humor can introduce errors into the assessment of aqueous humor kinetics.

For the posterior segment of the eye, MRI can be used to non-invasively examine the blood-retina barrier and vitreous fluidity (93-96). Dysfunction in the blood-retina barrier can be studied with MRI by using a contrast agent such as $GdDTPA^{2-}$, delivered intravenously to the retinal blood vessels, and monitoring its diffusion (leakage) into the vitreous humor. For example, this MRI method has been used to quantify the permeability of the blood-retina barrier to the contrast agent after the induction of lesions on the retina (96-98). Similar studies have determined the effects of endophthalmitis and diabetic retinopathy on the blood-retina barrier function (99,100). In these studies, the leakiness and time to restoration of the blood-retina barrier were monitored in endotoxin-induced endophthalmitis and experimental diabetic retinopathy, respectively. Ischemia-induced blood-retina barrier lesions have also been examined with MRI (101). Together, these studies demonstrate that MRI is a technique with potential for assessment of ocular drug-delivery systems in the treatment of posterior eye diseases related to blood-retina barrier function.

Indirect measurement of drug effects by MRI

The effectiveness of a drug-delivery system in the treatment of ocular diseases can be studied indirectly by MRI as described in the preceding section. In this case, MRI can be used to non-invasively study the effects of drugs or therapeutic interventions on a disease state that affects the blood-aqueous or blood-retina barriers. For example, Berkowitz *et al*. (100) used $GdDTPA^{2-}$ and dynamic contrast-enhanced MRI to measure the permeability of the blood/retina barrier in experimental diabetic retinopathy in rats and suggested that the MRI method can provide useful evaluation of ocular drug delivery or drug treatment efficacy because of its non-invasiveness. Wilson *et al*. (102) used MRI to evaluate the effects of sub-Tenon and intravitreal injections of triamcinolone acetonide on photocoagulation-induced blood-retina barrier breakdown in rabbit eyes. In another study, the effects of intravitreal injection of triamcinolone acetonide on an experimental proliferative vitreoretinopathy model were determined by quantifying the leakage of contrast agent through the blood-retina barrier with MRI (103). Monitoring of blood ocular barriers such as the blood-retina barrier with MRI has also allowed the study of the delivery of VEGF from a poly(L-lactide-co-glycolide)-based intravitreal implant (104) and the effects of intraocular irrigating solutions in vitrectomy (105).

Direct measurement of contrast agents as drug surrogates

This section will review MRI studies of the mechanisms of ocular drug delivery using contrast agents as drug surrogates *in vivo*. The distribution and clearance of these probes have been determined directly with MRI, and the ocular drug-delivery methods evaluated. Rabbits were the animal model used in all these studies, and, in some cases, postmortem rabbits and freshly enucleated eyes were also used.

One of the first MRI studies to directly evaluate the distribution of a contrast ion probe delivered into the eye with an ocular drug-delivery method was the investigation of the pathways of electric current in transcorneal and transscleral iontophoresis (73). In the same study, the distribution of the probe ion in the vitreous humor after intravitreal injection was also monitored, and the diffusion coefficient of the ion in the vitreous humor was determined. Subsequently, factors affecting transscleral iontophoretic delivery, such as electric current level, position, and duration of iontophoresis application, were evaluated (106), and the flux-enhancing mechanisms of transscleral iontophoresis, such as ocular barrier alterations, were examined (107). In these studies, the contrast agents were found to be delivered primarily into the anterior segment of the eye via the ciliary body (pars plana) as the least resistive route when the sclera near the limbus was the application site. A noteworthy point about these studies is the use of contrast agents at concentrations significantly higher than the concentration of the maximum MRI signal in the MRI signal vs concentration curve (e.g., see Fig. 2). A range of contrast agent concentrations was used in the experiments, so the region in the signal vs concentration plot representing the concentration of the contrast agent can be identified in the analysis of the signals in the MR images.

In another study, Kim *et al*. (53,108) used MRI to investigate drug delivery to the posterior segment of the eye from a sustained-release implant placed on the episclera and in the vitreous cavity using a contrast agent. The concentration profile, clearance, and pharmacokinetics of the contrast agent in the eye were modeled. The pharmacokinetic data suggest that drug elimination from the subconjunctival space into the conjunctival lymphatics created a significant transscleral barrier for intraocular delivery of the contrast agent. Episcleral implants were therefore concluded not to be effective in delivering the contrast agent into the vitreous humor.

To investigate the effectiveness of transscleral delivery of polar compounds via the subconjunctival route, Li *et al*. (109) determined the distribution and clearance of contrast agents in the subconjunctival space after subconjunctival injection with MRI. It was found that subconjunctival injection did not provide significant penetration of the contrast agents into the eye, and the pars plicata/pars plana was the least resistant pathway for passive transscleral drug delivery. The change in the volume of the subconjunctival pocket over time after the injection was also determined. A more recent study of the subconjunctival route with MRI examined the distribution and clearance of a macromolecule, Gd-labeled albumin, after subconjunctival injection (110). Jockovich *et al*. (111) recently used MRI to localize and monitor an anecortave acetate formulation administered periocularly to the eye with a posterior juxtascleral injection technique. The clearance behind the eye of a contrast agent in the formulation was examined with MRI in an attempt to determine the distribution and location of the drug over time after the injection.

MRI has also been used to study subconjunctival infusion into the episcleral space at the back of the eye and intrascleral infusion into the suprachoroidal space (112). A contrast agent was infused by inserting catheters into the subconjunctival or intrascleral space, and the 3D distribution of the contrast agent and its clearance in the eye were monitored with MRI. Similar to the findings in the above studies, no contrast agent was detected at the back of the eye as a result of subconjunctival infusion because of the resistive transscleral barriers. On the other hand, the contrast agent was found in the expanded suprachoroidal space of the posterior segment of the eye after intrascleral infusion.

CONCLUSION

This review has illustrated the usefulness of MRI in ocular drug-delivery study and for testing ocular drug-delivery methods. The advantages of MRI for studying the mechanisms of ocular

drug-delivery methods, such as the flux-enhancing mechanisms of ocular iontophoresis, the release kinetics from an ocular implant, the least resistive route for transscleral penetration, the locations of the periocular and intraocular depots in periocular, intrascleral, and intravitreal injections and infusions, and the delivery from and clearance in these depots, are demonstrated. Without MRI, such information would be difficult to obtain in traditional pharmacokinetic studies involving dissection of the eye.

FUTURE PERSPECTIVE

Monitoring of the distribution of compounds in the eye is essential for the development of ocular drug-delivery methods. Non-invasive pharmacokinetic studies are the key to providing crucial information that cannot be obtained from traditional ocular pharmacokinetic studies in animals and humans. MRI is a technique that can be used in ocular drug-delivery research. It is a promising complementary technique to traditional methods. With the advances in MRI technology and the emergence of more sophisticated MRI systems, this method will continue to help pharmaceutical scientists to gain insights into the mechanisms of ocular drug delivery and to develop effective ocular drug-delivery methods. However, a main drawback of MRI is the limitation of the drug candidates and drug-delivery systems that can be visualized. Only contrast agents and drugs with magnetic atoms such as fluorine can be studied using this technique. In summary, MRI has provided new possibilities in ocular drug-delivery research and will continue to assist the development and testing of ocular drug delivery.

Acknowledgements

We thank Sarah A. Molokhia and Stephanie H. Kim for providing the MR data in this review, and Drs Hyuncheol Kim, Jinsong Hao, and Yanhui Zhang for their help. Some unpublished MR data were obtained from studies supported by NIH Grant EY 015181.

Abbreviations used

GRE, gradient echo; RF, radio frequency; ROI, region of interest; SE, spin echo; SNR, signal-to-noise ratio; VEGF, vascular endothelial growth factor.

REFERENCES

1. Bauer NJ, Motamedi M, Wicksted JP, March WF, Webers CA, Hendrikse F. Non-invasive assessment of ocular pharmacokinetics using Confocal Raman Spectroscopy. J. Ocul. Pharmacol. Ther 1999;15:123–134. [PubMed: 10229490]
2. Szymanski-Exner A, Stowe NT, Salem K, Lazebnik R, Haaga JR, Wilson DL, Gao J. Noninvasive monitoring of local drug release using X-ray computed tomography: optimization and *in vitro/in vivo* validation. J. Pharm. Sci 2003;92:289–296. [PubMed: 12532379]
3. Mader K, Bacic G, Domb A, Elmalak O, Langer R, Swartz HM. Noninvasive *in vivo* monitoring of drug release and polymer erosion from biodegradable polymers by EPR spectroscopy and NMR imaging. J. Pharm. Sci 1997;86:126–134. [PubMed: 9002472]
4. Massoud TF, Paulmurugan R, De A, Ray P, Gambhir SS. Reporter gene imaging of protein-protein interactions in living subjects. Curr. Opin. Biotechnol 2007;18:31–37. [PubMed: 17254764]
5. Rudin M, Weissleder R. Molecular imaging in drug discovery and development. Nat. Rev. Drug Discov 2003;2:123–131. [PubMed: 12563303]
6. Yang DJ, Kim EE, Inoue T. Targeted molecular imaging in oncology. Ann. Nucl. Med 2006;20:1–11. [PubMed: 16485568]
7. Richardson JC, Bowtell RW, Mader K, Melia CD. Pharmaceutical applications of magnetic resonance imaging (MRI). Adv. Drug Deliv. Rev 2005;57:1191–1209. [PubMed: 15935869]

8. Rudin M, Beckmann N, Porszasz R, Reese T, Bochelen D, Sauter A. *In vivo* magnetic resonance methods in pharmaceutical research: current status and perspectives. NMR Biomed 1999;12:69–97. [PubMed: 10392805]
9. Beckmann N, Mueggler T, Allegrini PR, Laurent D, Rudin M. From anatomy to the target: contributions of magnetic resonance imaging to preclinical pharmaceutical research. Anat. Rec 2001;265:85–100. [PubMed: 11323771]
10. Wilson CG. In-vivo monitoring of dosage forms. J. Pharm. Pharmacol 1998;50:383–386. [PubMed: 9625482]
11. Marciani L, Wickham MS, Bush D, Faulks R, Wright J, Fillery-Travis AJ, Spiller RC, Gowland PA. Magnetic resonance imaging of the behaviour of oil-in-water emulsions in the gastric lumen of man. Br. J. Nutr 2006;95:331–339. [PubMed: 16469150]
12. Viglianti BL, Abraham SA, Michelich CR, Yarmolenko PS, MacFall JR, Bally MB, Dewhirst MW. *In vivo* monitoring of tissue pharmacokinetics of liposome/drug using MRI: illustration of targeted delivery. Magn. Reson. Med 2004;51:1153–1162. [PubMed: 15170835]
13. Port RE, Schuster C, Port CR, Bachert P. Simultaneous sustained release of fludarabine monophosphate and Gd-DTPA from an interstitial liposome depot in rats: potential for indirect monitoring of drug release by magnetic resonance imaging. Cancer Chemother Pharmacol 2006;58:607–617. [PubMed: 16506037]
14. Chen HH, Le Visage C, Qiu B, Du X, Ouwerkerk R, Leong KW, Yang X. MR imaging of biodegradable polymeric microparticles: a potential method of monitoring local drug delivery. Magn. Reson. Med 2005;53:614–620. [PubMed: 15723408]
15. Wang Y, Ye F, Jeong EK, Sun Y, Parker DL, Lu ZR. Noninvasive visualization of pharmacokinetics, biodistribution and tumor targeting of poly[*N*-(2-hydroxypropyl)methacrylamide] in mice using contrast enhanced MRI. Pharm. Res 2007;24:1208–1216. [PubMed: 17387601]
16. Ye F, Ke T, Jeong EK, Wang X, Sun Y, Johnson M, Lu ZR. Noninvasive visualization of *in vivo* drug delivery of poly(L-glutamic acid) using contrast-enhanced MRI. Mol. Pharm 2006;3:507–515. [PubMed: 17009849]
17. Kayyem JF, Kumar RM, Fraser SE, Meade TJ. Receptor-targeted co-transport of DNA and magnetic resonance contrast agents. Chem. Biol 1995;2:615–620. [PubMed: 9383466]
18. Chowning SL, Susil RC, Krieger A, Fichtinger G, Whitcomb LL, Atalar E. A preliminary analysis and model of prostate injection distributions. Prostate 2006;66:344–357. [PubMed: 16302267]
19. Christodoulou P, Doxas PG, Papadakis CE, Prassopoulos P, Maris T, Helidonis ES. Transtympanic iontophoresis of gadopentetate dimeglumine: preliminary results. Otolaryngol. Head Neck Surg 2003;129:408–413. [PubMed: 14574297]
20. Maris TG, Prassopoulos P, Papanikolaou N, Christodoulou P, Doxas PG, Helidonis ES, Gourtsoyiannis N. Transtympanic iontophoresis with a biocompatible paramagnetic solution at MR imaging: experimental feasibility study in rabbits. Radiology 2002;223:689–694. [PubMed: 12034936]
21. Barnhart KT, Pretorius ES, Timbers K, Shera D, Shabbout M, Malamud D. *In vivo* distribution of a vaginal gel: MRI evaluation of the effects of gel volume, time and simulated intercourse. Contraception 2004;70:498–505. [PubMed: 15541413]
22. Schoenwald, R. Textbook of Ocular Pharmacology. Zimmerman, T.; Kooner, K.; Sharir, M.; Fechtner, R., editors. Lippincott-Raven; Philadelphia: 1997.
23. Worakul N, Robinson J. Ocular pharmacokinetics/pharmacodynamics. Eur. J. Pharm. Biopharm 1997;44:71–83.
24. Cekic O, Batman C, Yasar U, Basci NE, Bozkurt A, Kayaalp SO. Comparison of aqueous humour and vitreous humour levels of two 0.3% ciprofloxacin eyedrops. Can. J. Ophthalmol 1998;33:373–376. [PubMed: 9885752]
25. Sakamoto H, Sakamoto M, Hata Y, Kubota T, Ishibashi T. Aqueous and vitreous penetration of levofloxacin after topical and/or oral administration. Eur. J. Ophthalmol 2007;17:372–376. [PubMed: 17534819]
26. Weijtens O, Feron EJ, Schoemaker RC, Cohen AF, Lentjes EG, Romijn FP, van Meurs JC. High concentration of dexamethasone in aqueous and vitreous after subconjunctival injection. Am. J. Ophthalmol 1999;128:192–197. [PubMed: 10458175]

27. Weijtens O, Schoemaker RC, Romijn FP, Cohen AF, Lentjes EG, van Meurs JC. Intraocular penetration and systemic absorption after topical application of dexamethasone disodium phosphate. Ophthalmology 2002;109:1887–1891. [PubMed: 12359610]
28. Ghate D, Edelhauser HF. Ocular drug delivery. Expert Opin. Drug Deliv 2006;3:275–287. [PubMed: 16506953]
29. Urtti A. Challenges and obstacles of ocular pharmacokinetics and drug delivery. Adv. Drug Deliv. Rev 2006;58:1131–1135. [PubMed: 17097758]
30. Davies NM. Biopharmaceutical considerations in topical ocular drug delivery. Clin. Exp. Pharmacol Physiol 2000;27:558–562. [PubMed: 10874518]
31. Mainardes RM, Urban MC, Cinto PO, Khalil NM, Chaud MV, Evangelista RC, Gremiao MP. Colloidal carriers for ophthalmic drug delivery. Curr. Drug Targets 2005;6:363–371. [PubMed: 15857294]
32. Mietz H, Diestelhorst M, Rump AF, Theisohn M, Klaus W, Krieglstein GK. Ocular concentrations of mitomycin C using different delivery devices. Ophthalmologica 1998;212:37–42. [PubMed: 9438583]
33. Taravella MJ, Balentine J, Young DA, Stepp P. Collagen shield delivery of ofloxacin to the human eye. J. Cataract Refract Surg 1999;25:562–565. [PubMed: 10198864]
34. Geroski DH, Edelhauser HF. Transscleral drug delivery for posterior segment disease. Adv. Drug Deliv. Rev 2001;52:37–48. [PubMed: 11672874]
35. Duvvuri S, Majumdar S, Mitra AK. Drug delivery to the retina: challenges and opportunities. Expert Opin. Biol. Ther 2003;3:45–56. [PubMed: 12718730]
36. Geroski DH, Edelhauser HF. Drug delivery for posterior segment eye disease. Invest Ophthalmol. Vis. Sci 2000;41:961–964. [PubMed: 10752928]
37. Olsen TW, Feng X, Wabner K, Conston SR, Sierra DH, Folden DV, Smith ME, Cameron JD. Cannulation of the suprachoroidal space: a novel drug delivery methodology to the posterior segment. Am. J. Ophthalmol 2006;142:777–787. [PubMed: 16989764]
38. Raghava S, Hammond M, Kompella UB. Periocular routes for retinal drug delivery. Expert Opin. Drug Deliv 2004;1:99–114. [PubMed: 16296723]
39. Chang DF, Wong V. Two clinical trials of an intraocular steroid delivery system for cataract surgery. Trans. Am. Ophthalmol. Soc 1999;97:261–274. [PubMed: 10703128]discussion 274-269
40. Chang M, Dunn JP. Ganciclovir implant in the treatment of cytomegalovirus retinitis. Expert Rev. Med. Devices 2005;2:421–427. [PubMed: 16293081]
41. Jaffe GJ, Martin D, Callanan D, Pearson PA, Levy B, Comstock T. Fluocinolone acetonide implant (Retisert) for noninfectious posterior uveitis: thirty-four-week results of a multicenter randomized clinical study. Ophthalmology 2006;113:1020–1027. [PubMed: 16690128]
42. Kodama M, Numaga J, Yoshida A, Kaburaki T, Oshika T, Fujino Y, Wu GS, Rao NA, Kawashima H. Effects of a new dexamethasone- delivery system (Surodex) on experimental intraocular inflammation models. Graefes Arch. Clin. Exp. Ophthalmol 2003;241:927–933. [PubMed: 14652765]
43. Regillo CD, D'Amico DJ, Mieler WF, Schneebaum C, Beasley CH, Sullins GT. Clinical safety profile of posterior juxtascleral depot administration of anecortave acetate 15 mg suspension as primary therapy or adjunctive therapy with photodynamic therapy for treatment of wet age-related macular degeneration. Surv. Ophthalmol 2007;52:S70–78. [PubMed: 17240259]
44. Halhal M, Renard G, Courtois Y, BenEzra D, Behar-Cohen F. Iontophoresis: from the lab to the bed side. Exp. Eye Res 2004;78:751–757. [PubMed: 15106955]
45. Missel PJ. Finite and infinitesimal representations of the vasculature: ocular drug clearance by vascular and hydraulic effects. Ann. Biomed. Eng 2002;30:1128–1139. [PubMed: 12502224]
46. Maurice DM. Review: practical issues in intravitreal drug delivery. J. Ocul. Pharmacol. Ther 2001;17:393–401. [PubMed: 11572470]
47. Prausnitz MR, Noonan JS. Permeability of cornea, sclera, and conjunctiva: a literature analysis for drug delivery to the eye. J. Pharm. Sci 1998;87:1479–1488. [PubMed: 10189253]
48. Ranta VP, Urtti A. Transscleral drug delivery to the posterior eye: prospects of pharmacokinetic modeling. Adv. Drug Deliv. Rev 2006;58:1164–1181. [PubMed: 17069929]

49. Robinson MR, Lee SS, Kim H, Kim S, Lutz RJ, Galban C, Bungay PM, Yuan P, Wang NS, Kim J, Csaky KG. A rabbit model for assessing the ocular barriers to the transscleral delivery of triamcinolone acetonide. Exp. Eye Res 2006;82:479–487. [PubMed: 16168412]
50. Deoni SC, Rutt BK, Peters TM. Rapid combined T_1 and T2 mapping using gradient recalled acquisition in the steady state. Magn. Reson. Med 2003;49:515–526. [PubMed: 12594755]
51. Liu, X.; Feng, Y.; Lu, ZR.; Jeong, EK. Rapid simultaneous data acquisition of T_1 and T2 mapping, using multishot EPI and automated variations of TR and TE at 3T; Joint Annual Meeting ISMRM-ESMRMB; Berlin, Germany. 2007; p. 1787
52. Friedrich S, Cheng YL, Saville B. Finite element modeling of drug distribution in the vitreous humor of the rabbit eye. Ann. Biomed. Eng 1997;25:303–314. [PubMed: 9084836]
53. Kim H, Lizak MJ, Tansey G, Csaky KG, Robinson MR, Yuan P, Wang NS, Lutz RJ. Study of ocular transport of drugs released from an intravitreal implant using magnetic resonance imaging. Ann. Biomed. Eng 2005;33:150–164. [PubMed: 15771269]
54. Yu JX, Kodibagkar VD, Cui W, Mason RP. ^{19}F: a versatile reporter for non-invasive physiology and pharmacology using magnetic resonance. Curr. Med. Chem 2005;12:819–848. [PubMed: 15853714]
55. Campbell GD, Ramaprasad S, Olsen KM, Tryka AF, Komoroski RA, Blaszczak LC, Parr Tr Jr. Comparison of the *in vivo* and *in vitro* nuclear magnetic resonance detection of trifluoromethyl penicillin V in rats. J. Pharm. Sci 1993;82:48–51. [PubMed: 8429491]
56. Griffiths JR, McIntyre DJ, Howe FA, McSheehy PM, Ojugo ASE, Rodrigues LM, Wadsworth P, Price NM, Lofts F, Nicholson G, Smid K, Noordhuis P, Peters GJ, Stubbs M. Issues of normal tissue toxicity in patient and animal studies: effect of carbogen breathing in rats after 5-fluorouracil treatment. Acta Oncol 2001;40:609–614. [PubMed: 11669333]
57. Fishman JE, Joseph PM, Floyd TF, Mukherji B, Sloviter HA. Oxygen-sensitive ^{19}F NMR imaging of the vascular system *in vivo*. Magn. Reson. Imaging 1987;5:279–285. [PubMed: 3657400]
58. Hashimoto T, Ikehira H, Fukuda H, Ueshima Y, Tateno Y. Study of biodistribution of enflurane in rats with *in vivo*^{19}F MRI. Magn. Reson. Imaging 1991;9:577–581. [PubMed: 1779729]
59. Brix G, Bellemann ME, Haberkorn U, Gerlach L, Lorenz WJ. Assessment of the biodistribution and metabolism of 5-fluorouracil as monitored by $_{18}$F PET and $_{19}$F MRI: a comparative animal study. Nucl. Med. Biol 1996;23:897–906. [PubMed: 8971857]
60. Gewiese BK, Noske W, Schilling AM, Stiller DA, Wolf KJ, Foerster MH. Human eye: visualization of perfluorodecalin with F-19 MR imaging. Radiology 1992;185:131–133. [PubMed: 1523296]
61. Midelfart A, Dybdahl A, N MU, Sitter B, Gribbestad IS, Krane J. Dexamethasone and dexamethasone phosphate detected by ^{1}H and ^{19}F NMR spectroscopy in the aqueous humour. Exp. Eye Res 1998;66:327–337. [PubMed: 9533860]
62. Koenig SH, Brown RD 3rd, Adams D, Emerson D, Harrison CG. Magnetic field dependence of 1/T_1 of protons in tissue. Invest Radiol 1984;19:76–81. [PubMed: 6533107]
63. Kang YS, Gore JC, Armitage IM. Studies of factors affecting the design of NMR contrast agents: manganese in blood as a model system. Magn. Reson. Med 1984;1:396–409. [PubMed: 6443783]
64. Ishimori Y, Yamada K, Kimura H, Fujiwara Y, Yamaguchi I, Monma M, Uematsu H. Correction of inhomogeneous RF field using multiple SPGR signals for high-field spin-echo MRI. Magn. Reson. Med. Sci 2007;6:67–73. [PubMed: 17690536]
65. Nagy Z, Weiskopf N, Alexander DC, Deichmann R. A method for improving the performance of gradient systems for diffusion-weighted MRI. Magn. Reson. Med 2007;58:763–768. [PubMed: 17899604]
66. Quesson B, de Zwart JA, Moonen CT. Magnetic resonance temperature imaging for guidance of thermotherapy. J. Magn. Reson. Imaging 2000;12:525–533. [PubMed: 11042633]
67. Crank, J. The Mathematics of Diffusion. Oxford University Press; New York: 1980.
68. Lauterbur PC. Image formation by induced local interactions. Examples employing nuclear magnetic resonance. Nature 1973;242, 5394:190–191.
69. Bock NA, Silva AC. Manganese: a unique neuron imaging contrast agent. Future Neurol 2007;2:297–305.
70. Kreft BP, Baba Y, Tanimoto A, Finn JP, Stark DD. Orally administered manganese chloride: enhanced detection of hepatic tumors in rats. Radiology 1993;186:543–548. [PubMed: 8421762]

71. Watanabe T, Michaelis T, Frahm J. Mapping of retinal projections in the living rat using high-resolution 3D gradient-echo MRI with Mn^{2+}-induced contrast. Magn. Reson. Med 2001;46:424–429. [PubMed: 11550231]
72. Pautler RG, Mongeau R, Jacobs RE. *In vivo* trans-synaptic tract tracing from the murine striatum and amygdala utilizing manganese enhanced MRI (MEMRI). Magn. Reson. Med 2003;50:33–39. [PubMed: 12815676]
73. Li SK, Jeong EK, Hastings MS. Magnetic resonance imaging study of current and ion delivery into the eye during transscleral and transcorneal iontophoresis. Invest Ophthalmol. Vis. Sci 2004;45:1224–1231. [PubMed: 15037591]
74. Dyatlova, N.; Temkina, V.; Popov, K. Present-day aspects of complex on coordination chemistry. In: Buslaev, Y., editor. Complex Formation and Stereochemistry of Coordination Compounds. Nova Science; New York: 1996. p. 1-48.
75. Tweedle MF, Hagan JJ, Kumar K, Mantha S, Chang CA. Reaction of gadolinium chelates with endogenously available ions. Magn. Reson. Imaging 1991;9:409–415. [PubMed: 1881260]
76. Rezai KA, Lappas A, Kohen L, Wiedemann P, Heimann K. Comparison of tight junction permeability for albumin in iris pigment epithelium and retinal pigment epithelium *in vitro*. Graefes Arch. Clin. Exp. Ophthalmol 1997;235:48–55. [PubMed: 9034842]
77. Tomita M, Hayashi M, Awazu S. Absorption-enhancing mechanism of EDTA, caprate, and decanoylcarnitine in Caco-2 cells. J. Pharm. Sci 1996;85:608–611. [PubMed: 8773957]
78. Runge VM, Clanton JA, Herzer WA, Gibbs SJ, Price AC, Partain CL, James AE Jr. Intravascular contrast agents suitable for magnetic resonance imaging. Radiology 1984;153:171–176. [PubMed: 6433402]
79. Kobayashi H, Brechbiel MW. Dendrimer-based nanosized MRI contrast agents. Curr. Pharm. Biotechnol 2004;5:539–549. [PubMed: 15579043]
80. Torchilin VP. PEG-based micelles as carriers of contrast agents for different imaging modalities. Adv. Drug Deliv. Rev 2002;54:235–252. [PubMed: 11897148]
81. Lauffer RB, Brady TJ, Brown RD 3rd, Baglin C, Koenig SH. $1/T_1$ NMRD profiles of solutions of Mn^{2+} and Gd^{3+} protein-chelate conjugates. Magn. Reson. Med 1986;3:541–548. [PubMed: 3747815]
82. Li Z, Li W, Li X, Pei F, Li Y, Lei H. The gadolinium complexes with polyoxometalates as potential MRI contrast agents. Magn. Reson. Imaging 2007;25:412–417. [PubMed: 17371733]
83. Dzik-Jurasz AS, Wolber J, Prock T, Collins DJ, Leach MO, Rowland IJ. The quantitative ^{19}F-imaging of albumin at 1.5 T: a potential in-vivo tool. Magn. Reson. Imaging 2001;19:839–844. [PubMed: 11551725]
84. Artemov D, Mori N, Okollie B, Bhujwalla ZM. MR molecular imaging of the Her-2/neu receptor in breast cancer cells using targeted iron oxide nanoparticles. Magn. Reson. Med 2003;49:403–408. [PubMed: 12594741]
85. Bulte JW, Kraitchman DL. Iron oxide MR contrast agents for molecular and cellular imaging. NMR Biomed 2004;17:484–499. [PubMed: 15526347]
86. Jung CW, Jacobs P. Physical and chemical properties of super-paramagnetic iron oxide MR contrast agents: ferumoxides, ferumoxtran, ferumoxsil. Magn. Reson. Imaging 1995;13:661–674. [PubMed: 8569441]
87. Kolodny NH, Freddo TF, Lawrence BA, Suarez C, Bartels SP. Contrast-enhanced magnetic resonance imaging confirmation of an anterior protein pathway in normal rabbit eyes. Invest Ophthalmol. Vis. Sci 1996;37:1602–1607. [PubMed: 8675403]
88. Cheng HM, Kwong KK, Xiong J, Chang C. GdDTPA-enhanced magnetic resonance imaging of the aqueous flow in the rabbit eye. Magn. Reson. Med 1991;17:237–243. [PubMed: 2067398]
89. Cheng HM, Kwong KK, Xiong J, Woods BT. Visualization of water movement in the living rabbit eye. Graefes Arch. Clin. Exp. Ophthalmol 1992;230:62–65. [PubMed: 1547970]
90. Wu JC, Jesmanowicz A, Hyde JS. Anterior segment high resolution MRI: aqueous humor dynamics observed using contrast agents. Exp. Eye Res 1992;54:145–148. [PubMed: 1541333]
91. Bert RJ, Caruthers SD, Jara H, Krejza J, Melhem ER, Kolodny NH, Patz S, Freddo TF. Demonstration of an anterior diffusional pathway for solutes in the normal human eye with high spatial resolution

contrast-enhanced dynamic MR imaging. Invest Ophthalmol. Vis. Sci 2006;47:5153–5162. [PubMed: 17122097]

92. Freddo TF, Patz S, Arshanskiy Y. Pilocarpine's effects on the blood-aqueous barrier of the human eye as assessed by high-resolution, contrast magnetic resonance imaging. Exp. Eye Res 2006;82:458–464. [PubMed: 16169551]
93. Berkowitz BA, Wilson CA, Tofts PS, Peshock RM. Effect of vitreous fluidity on the measurement of blood-retinal barrier permeability using contrast-enhanced MRI. Magn. Reson. Med 1994;31:61–66. [PubMed: 8121271]
94. Plehwe WE, McRobbie DW, Lerski RA, Kohner EM. Quantitative magnetic resonance imaging in assessment of the blood-retinal barrier. Invest Ophthalmol. Vis. Sci 1988;29:663–670. [PubMed: 3366561]
95. Berkowitz BA, Tofts PS, Sen HA, Ando N, de Juan E Jr. Accurate and precise measurement of blood-retinal barrier breakdown using dynamic Gd-DTPA MRI. Invest Ophthalmol. Vis. Sci 1992;33:3500–3506. [PubMed: 1464496]
96. Sen HA, Berkowitz BA, Ando N, de Juan E Jr. *In vivo* imaging of breakdown of the inner and outer blood-retinal barriers. Invest Ophthalmol. Vis. Sci 1992;33:3507–3512. [PubMed: 1464497]
97. Berkowitz BA, Sato Y, Wilson CA, de Juan E. Blood-retinal barrier breakdown investigated by real-time magnetic resonance imaging after gadolinium-diethylenetriaminepentaacetic acid injection. Invest Ophthalmol. Vis. Sci 1991;32:2854–2860. [PubMed: 1917389]
98. Sato Y, Berkowitz BA, Wilson CA, de Juan E Jr. Blood-retinal barrier breakdown caused by diode vs argon laser endophoto-coagulation. Arch. Ophthalmol 1992;110:277–281. [PubMed: 1736878]
99. Metrikin DC, Wilson CA, Berkowitz BA, Lam MK, Wood GK, Peshock RM. Measurement of blood-retinal barrier breakdown in endotoxin-induced endophthalmitis. Invest Ophthalmol. Vis. Sci 1995;36:1361–1370. [PubMed: 7775114]
100. Berkowitz BA, Roberts R, Luan H, Peysakhov J, Mao X, Thomas KA. Dynamic contrast-enhanced MRI measurements of passive permeability through blood retinal barrier in diabetic rats. Invest Ophthalmol. Vis. Sci 2004;45:2391–2398. [PubMed: 15223822]
101. Wilson CA, Berkowitz BA, Funatsu H, Metrikin DC, Harrison DW, Lam MK, Sonkin PL. Blood-retinal barrier breakdown following experimental retinal ischemia and reperfusion. Exp. Eye Res 1995;61:547–557. [PubMed: 8654497]
102. Wilson CA, Berkowitz BA, Sato Y, Ando N, Handa JT, de Juan E Jr. Treatment with intravitreal steroid reduces blood-retinal barrier breakdown due to retinal photocoagulation. Arch. Ophthalmol 1992;110:1155–1159. [PubMed: 1497531]
103. Ando N, Sen HA, Berkowitz BA, Wilson CA, de Juan E Jr. Localization and quantitation of blood-retinal barrier breakdown in experimental proliferative vitreoretinopathy. Arch. Ophthalmol 1994;112:117–122. [PubMed: 8285878]
104. Alikacem N, Yoshizawa T, Nelson KD, Wilson CA. Quantitative MR imaging study of intravitreal sustained release of VEGF in rabbits. Invest Ophthalmol. Vis. Sci 2000;41:1561–1569. [PubMed: 10798677]
105. Garner WH, Scheib S, Berkowitz BA, Suzuki M, Wilson CA, Graff G. The effect of partial vitrectomy on blood-ocular barrier function in the rabbit. Curr. Eye Res 2001;23:372–381. [PubMed: 11910527]
106. Molokhia SA, Jeong EK, Higuchi WI, Li SK. Examination of penetration routes and distribution of ionic permeants during and after transscleral iontophoresis with magnetic resonance imaging. Int. J. Pharm 2007;335:46–53. [PubMed: 17236728]
107. Molokhia SA, Jeong EK, Higuchi WI, Li SK. Examination of barriers and barrier alteration in transscleral iontophoresis. J. Pharm. Sci. in press
108. Kim H, Robinson MR, Lizak MJ, Tansey G, Lutz RJ, Yuan P, Wang NS, Csaky KG. Controlled drug release from an ocular implant: an evaluation using dynamic three-dimensional magnetic resonance imaging. Invest Ophthalmol. Vis. Sci 2004;45:2722–2731. [PubMed: 15277497]
109. Li SK, Molokhia SA, Jeong EK. Assessment of subconjunctival delivery with model ionic permeants and magnetic resonance imaging. Pharm. Res 2004;21:2175–2184. [PubMed: 15648248]

110. Kim, SH.; Lutz, RJ.; Galban, CJ.; Wang, NS.; Csaky, KG. Analysis of drug elimination kinetics after subconjunctival injection using magnetic resonance imaging; ARVO Annual Meeting; 2007; p. B322Program 5785

111. Jockovich ME, Murray TG, Clifford PD, Moshfeghi AA. Posterior juxtascleral injection of anecortave acetate: magnetic resonance and echographic imaging and localization in rabbit eyes. Retina 2007;27:247–252. [PubMed: 17290209]

112. Kim SH, Galban CJ, Lutz RJ, Dedrick RL, Csaky KG, Lizak MJ, Wang NS, Tansey G, Robinson MR. Assessment of subconjunctival and intrascleral drug delivery to the posterior segment using dynamic contrast-enhanced magnetic resonance imaging. Invest Ophthalmol. Vis. Sci 2007;48:808–814. [PubMed: 17251481]

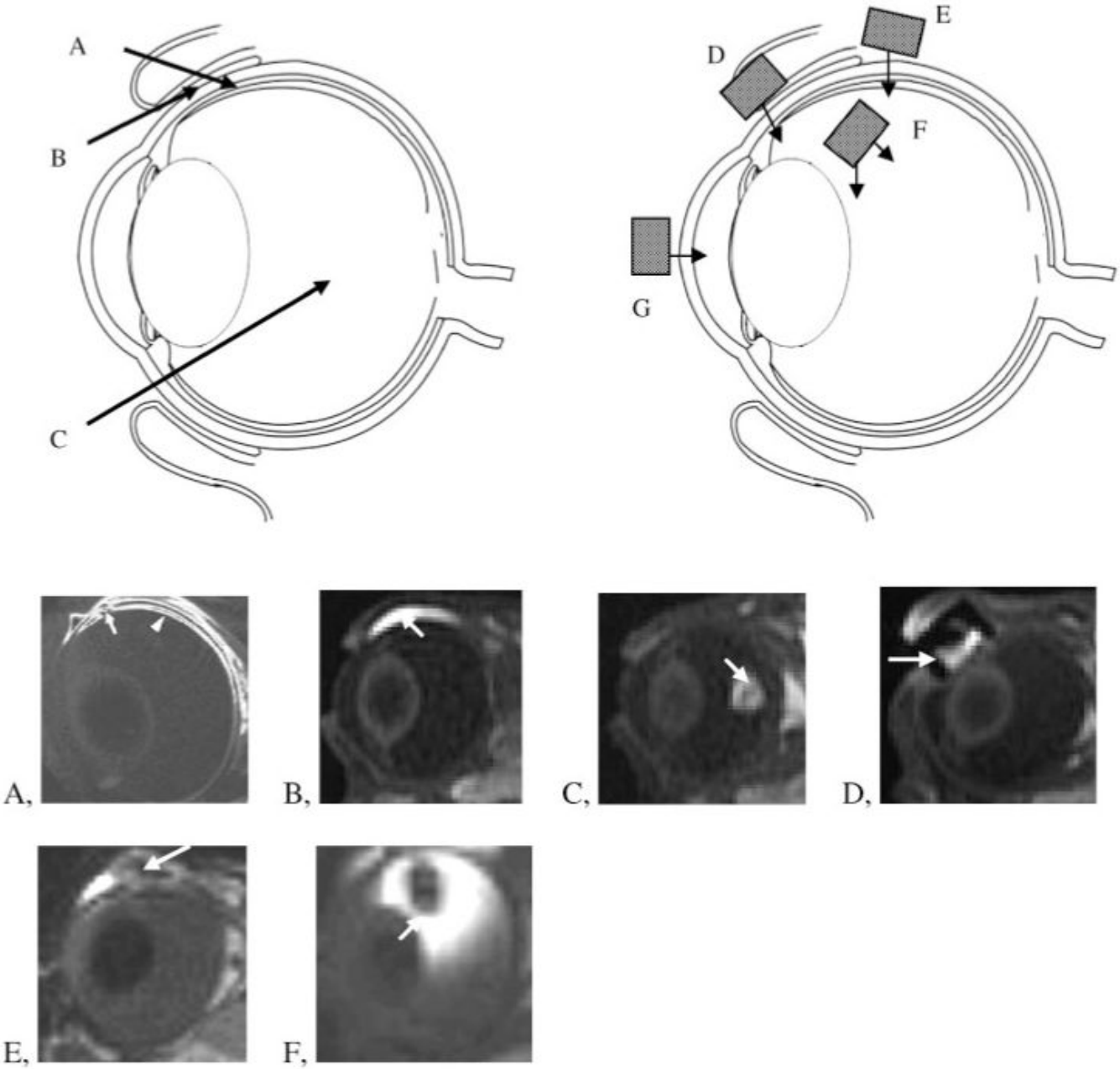

Figure 1.

(a) Examples of drug-delivery methods studied using MRI: A, intrascleral infusion or injection into the suprachoroidal space; B, subconjunctival injection; C, intravitreal injection; D, transscleral iontophoresis; E, episcleral implant; F, intravitreal implant; G, transcorneal iontophoresis. (b) Representative MR images of ocular drug delivery in rabbits: A, intrascleral infusion; B, subconjunctival injection; C, intravitreal injection; D, ocular iontophoresis; E, episcleral implant; F, intravitreal implant. The arrows indicate the sites of drug delivery or the drug-delivery systems. Images are obtained from previous studies at 1.5, 3, or 4.7 T (53,73, 108,109,112).

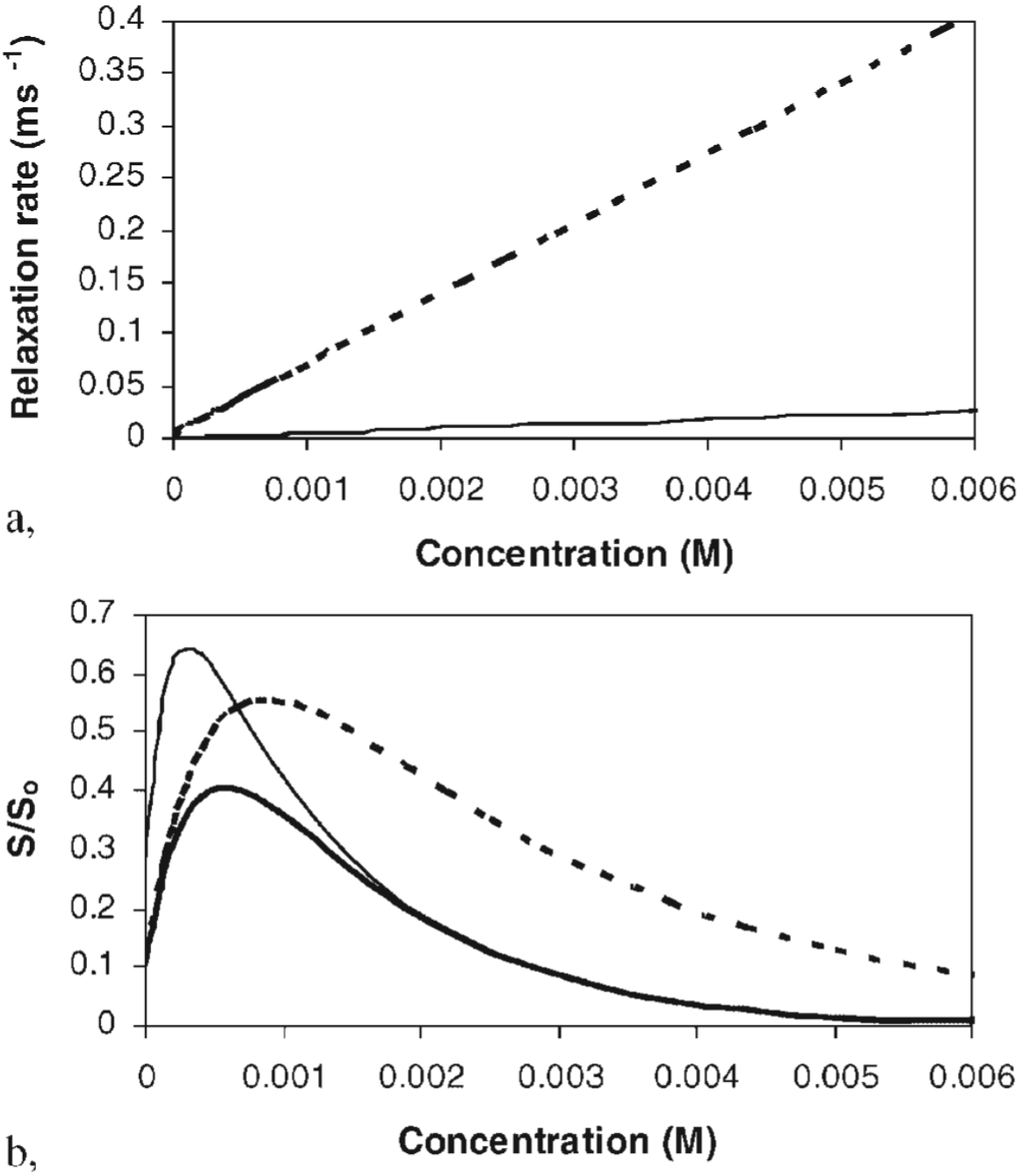

Figure 2.

(a) Relationships between relaxation rates and contrast agent concentration. In this example, data for Mn^{2+} in saline at 1.5 T are used. Lines: solid, T_1; dashed, T_2. (b) Relationships between the signal intensity normalized by S_o (i.e. S/S_o) and the concentration of contrast agent Mn^{2+}. Lines: thick solid, *TR* 400 ms, *TE* 12 ms; thin solid, *TR* 1200 ms, *TE* 12 ms; thick dashed, *TR* 400 ms, *TE*, 6 ms.

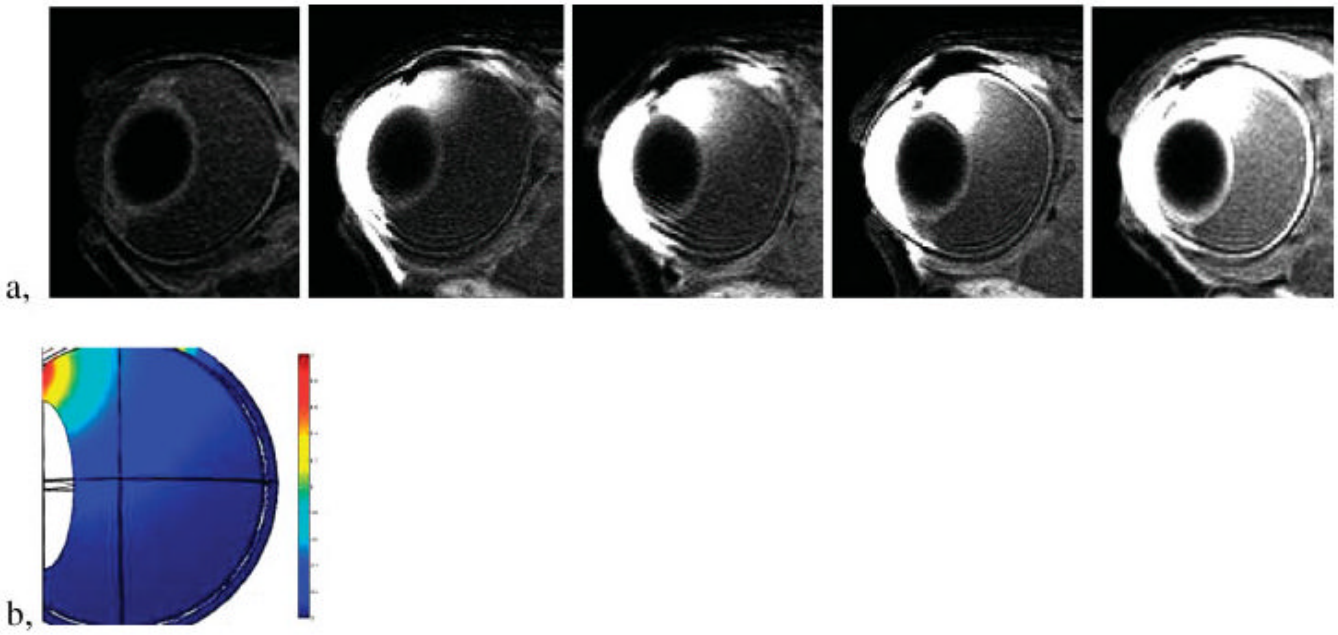

Figure 3.

Distribution of Mn^{2+} in the eye after 20 min of 3 mA transscleral iontophoresis applied on the sclera next to the limbus: (a), from left to right, control and at 1, 2, 3, and 11 h after iontophoresis application; (b) model simulation result of a finite element method using Comsol (Burlington, MA, USA) mimicking the 3 h MRI data. The MRI scans were performed with a 3 T Siemens clinical scanner.

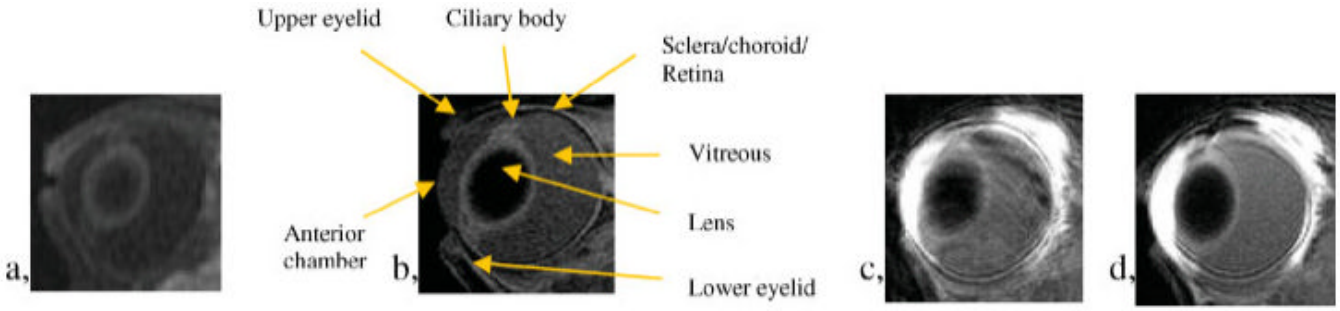

Figure 4.

MR images of rabbit eyes at (a) 0.47 mm × 0.47 mm × 2 mm resolution and (b) 0.3 mm × 0.3 mm × 1 mm resolution. The MRI scans were performed with 1.5 T GE clinical and 3 T Siemens clinical scanners with scan times of ~1.5 and 20 min for (a) and (b), respectively. MR images obtained in an ocular delivery study conducted with the 3 T Siemens clinical scanner (c) with motion artifacts in the phase-encoding direction and (d) without motion artifacts.

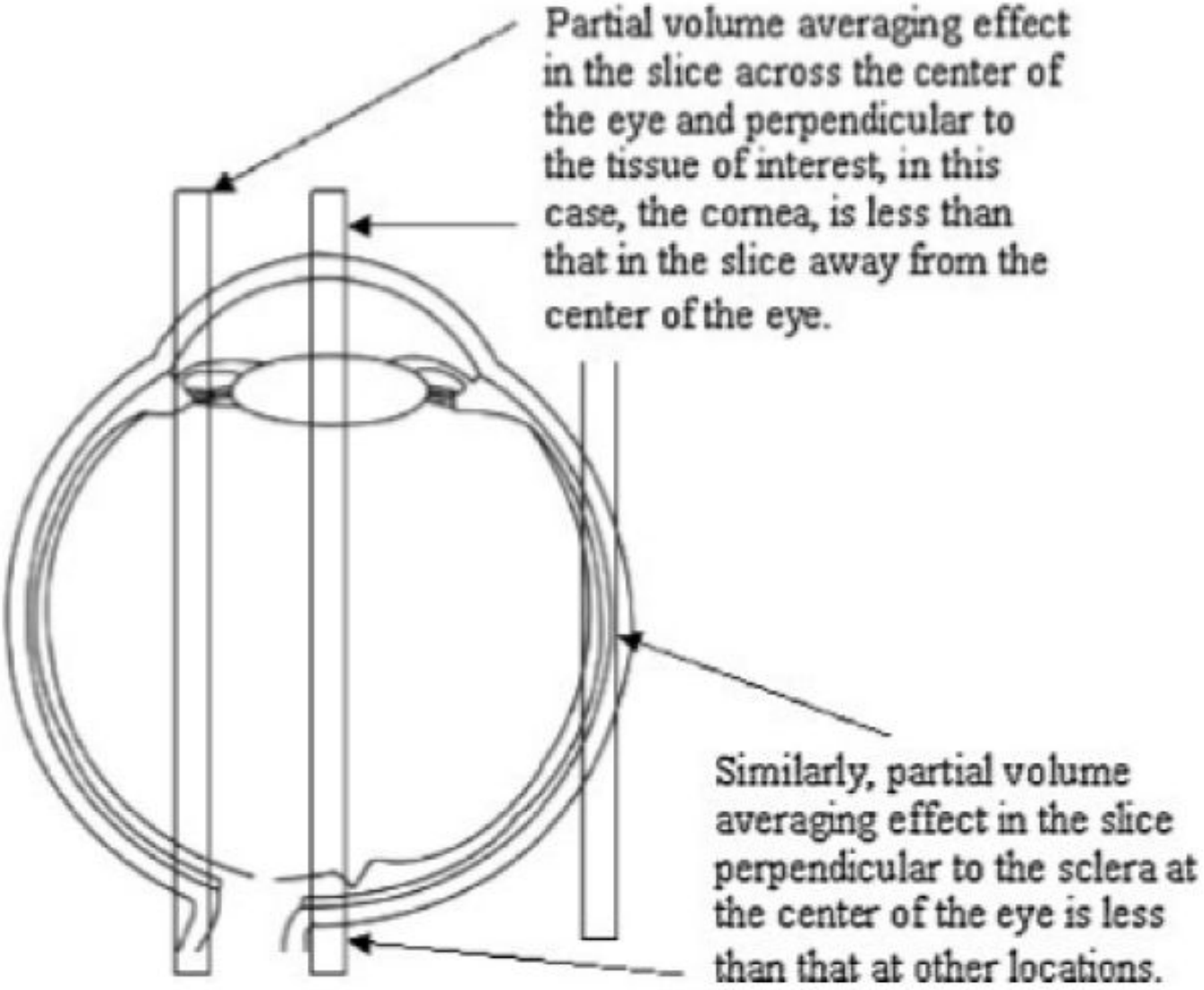

Figure 5.
Effects of partial-volume averaging in MRI ocular drug-delivery study.

Table 1

Summary of the advantages and limitations of the use of the MRI technique in ocular drug-delivery research and comparison with the traditional ocular pharmacokinetics method of eye enucleation and dissection

	MRI	Traditional pharmacokinetics
Type	Non-invasive	Invasive
Procedure	Continuous monitoring over time without killing the animal	Killing the animal and dissecting the eye at different time points
Molecule/drug	Can only monitor contrast agent or certain molecules. Selective monitoring	All types of molecules as long as tissue assay is available. Require assay development
Spatial resolution	Can monitor 3D distribution of small volume, but resolution may not be high enough to determine the concentration in thin tissues	Cannot evaluate 3D distribution of small finite volume, but can determine amount in small tissues (through dissection)
Temporal resolution	Limited by scan time, which is related to spatial resolution	Limited by the time of dissection. Tissue can be frozen to avoid molecule redistribution. Redistribution in tissue during dissection can be an issue.
Errors	Variability due to MRI hardware, experimental setup, and technique. Partial volume averaging effect. Relaxation times affected by tissue and microenvironment such as temperature and viscosity	Possible cross-contamination among tissues during dissection. Inherited errors from analytical techniques in tissue assay. Can be less variable than MRI
Sensitivity and detection limit	Relatively low compared with conventional assay techniques such as HPLC[a] and GC	High sensitivity and good limit of quantification to detect low concentration
Human clinical study	Possible with approved contrast agents and/or ^{19}F MRS/MRI of the fluorinated drug compound	Difficult and not feasible with healthy subjects
Resource and cost	Expensive equipment is required. Special hardware is sometimes needed, such as ^{19}F MR. Only a small number of animals is needed	Skillful researchers to perform precise dissection. Require a large number of animals

[a]HPLC, high-performance liquid chromatography; GC, gas chromatography.

Table 2

Possible contrast agents for ocular drug-delivery research using MRI

Type	Compounds
Small contrast ions	Mn^{2+}, Gd^{3+}
Small chelated contrast ions	Mn and Gd complexes: $MnEDTA^{2-}$, $GdDTPA^{2-}$, and $GdDOTA^{2-}$
Small contrast-labeled drugs	Not useful because it is difficult to retain the physicochemical properties of the drug for pharmacokinetic evaluations with the labeling of the large chelated contrast-ion complex
Iron oxide contrast agents	Iron oxide particles: superparamagnetic iron oxide nanoparticles
Contrast-labeled macromolecules	Peptides, oligonucleotides, proteins, RNA, DNA
Contrast-labeled synthetic polymers	Polyanions, polycations, and neutral polymers that resemble macromolecules or drug carriers
Contrast-labeled drug-delivery system	Nanoparticles, microspheres, micelles, liposomes, polymeric carriers for drug delivery

Table 3

Technicalities in MRI ocular drug-delivery study and their comparison: a summary

MRI pulse sequence	Spin-echo (SE) • straightforward T_1 and T_2 contrast • relatively poor SNR • long imaging time	Gradient-echo (GRE) • fast imaging using steady-state and low flip angle • local non-uniformity of magnetic field • mixed with T_1 and T_2* contrast
Signal to concentration calculation	T_1 and T_2 mappings to determine concentration • require model fitting of the data • not practical because of the long scan time • independent of hardware variability such as RF field uniformity	MR signal to concentration direct conversion via calibration • possible errors due to RF coil positioning • signal depends on both T_1 and T_2 • affected by hardware variability • direct approach
MRI parameters related to spatial resolution	Imaging field of view, readout matrix, slice thickness • determine spatial resolution vs SNR	Number of image slices • increases MRI coverage • too many slices will increase scan time
MRI parameters directly related to signal	*TR, TE* • determine T_1 or T_2 contrast • affect signal intensity • need *TR* and *TE* for optimal contrasts and acquisition efficiency	Signal averages • increase SNR • increase scan time and decrease temporal resolution
Coil	Surface coil • higher SNR • lacks signal homogeneity • variation due to inhomogeneous spatial sensitivity of coil	Volume coil • increased RF field homogeneity • increased signal uniformity • lower SNR from eye
MRI system	Clinical whole-body scanner • fits large animals • stable and well-tuned imaging sequences • limitation for high-resolution imaging • less friendly to custom-made hardware, such as RF coil for non-proton MRI/MRS • can be used for humans	Animal scanner • suitable for small animals • usually higher magnetic field • more hardware flexibility
Animal model	Large animals	Small animals such as rodents • easy to handle

NIH-PA Author Manuscript
NIH-PA Author Manuscript

	• may not fit into the bore of a scanner • can be difficult to handle • eye dimensions are more representative of human eye	• small eyes not representative of human eye
Contrast agent considerations	Physicochemical properties relative to the drug of interest • molecular size • molecular charge • lipophilicity	MR properties and biological effects • MR signal enhancement • specific tissue interactions • tissue binding • tissue MR signal and contrast concentration to MR signal calibration

Table 4

MRI methods for studying ocular drug delivery

	Measurement of physiological factors and variables	Indirect measurement of drug effects by MRI	Direct measurement of drugs or contrast agents as drug surrogates
Descriptions	• Studies unrelated to ocular drug delivery but provide information that can be used to predict or understand ocular drug delivery	• Monitoring of the pharmacodynamics and effects of the drug	• Drug-delivery study by monitoring the distribution and clearance of a contrast agent delivered into the eye from a drug-delivery system or method • Direct measurement of a fluorine-containing drug with ^{19}F
Examples	• Study of variables that affect drug distribution and clearance in the eye such as the flow of aqueous humor • Study of ocular tissue barriers such as the blood-aqueous barrier and blood-retina barrier	• Study of the effectiveness of a drug-delivery system or method by monitoring its effects • Evaluation of side effects to the eye tissues due to a drug-delivery system or method	• Monitoring of the distribution and clearance of a contrast agent with similar physicochemical properties to the drug • Monitoring of the location, distribution, and/or clearance of a contrast-labeled drug-delivery system